

Supporting Information

Bifunctional thioacetamide-mediated synthesis of few-layered MoOS_x nanosheet-modified CdS hollowspheres for efficient photocatalytic H₂ production

Siqin Tao,^a Wei Zhong,^a Yuxiao Chen,^a Feng Chen,^a Ping Wang,^a and Huogen Yu^{*ab}

^a *School of Chemistry, Chemical Engineering and Life Sciences, and State Key Laboratory of Silicate Materials for Architectures, Wuhan University of Technology, Wuhan 430070, PR China*

^b *Laboratory of Solar Fuel, Faculty of Materials Science and Chemistry, China University of Geosciences, Wuhan, 430070, PR China*

*Corresponding author. Tel: +86-27-87756662; Fax: +86-27-87879468;

E-mail: huogenyu@163.com

SI-1 Characterization

Fourier transform infrared spectra (FTIR) and Raman data were recorded utilizing Nexus FTIR Spectrophotometer and an INVIA spectrophotometer, respectively. Transmission electron microscopy (TEM) and elemental mapping images were applied on JEM-2100F, with a high angle annular dark field imaging (HAADF-STEM) and energy-dispersive X-ray spectrometer (Oxford Instruments, Britain). The morphology and structure features were analyzed by field emission scanning electron microscopy (FESEM, JSM-7500F) and X-ray diffraction (XRD, Rigaku, Japan) patterns. A KRATOA XSAM800 system was applied to acquire X-ray photoelectron spectroscopy (XPS) spectra and an ESCALAB 10 electron spectrometer was used to collect *in situ* X-ray photoelectron spectroscopy (XPS) spectra. For optical properties analysis, UV-vis diffuse reflectance spectra were utilized on a UV-2450 Shimadzu spectrophotometer. The time-resolved transient photoluminescence (TRPL) spectra were implemented on FLS920 fluorescence spectrophotometer.

SI-2 Photoelectrochemical experiments

Photoelectrochemical measurements were obtained on a CHI660E electrochemical workstation with a three-electrode cell within a nitrogen atmosphere in Na₂SO₄ (0.5 M) solution. The test equipment includes a Pt sheet as the counter electrode, an Ag/AgCl electrode as the reference electrode, and sample-loaded FTO glass as the working electrode. The sample-loaded FTO was prepared as follows: 10 mg of powder was dispersed into 2.5 mL of ethanol, and then, 2.5 mL of 1 wt % Nafion ethanol mixing solution was added, and finally the above mixture was uniformly mixed by ultrasonic for 30 min. The obtained FTO glass was dried at 50 °C for 12 h. During *i-t* curve measurements, a 420 nm, 3 W LED was used as the light source, and the open-circuit voltage (0.5 V) was used as the applied bias. For the EIS measurements, the frequency was applied in a range of 10⁻³ to 10⁶ Hz with an amplitude of 0.01 V. In the linear sweep voltammogram tests, the applied bias was used from -1.2 to -1.7 V.

SI-3 DFT computational methods

All the first principle calculations were carried out by using the Vienna Ab initio Simulation Package (VASP). Generalized gradient approximation (GGA) with Perdew-Burke-Ernzerhof (PBE) functional was selected to describe the exchange-correlation interaction. The energy cutoff and Monkhorst-Pack k-point meshes were set as 450 eV and $3 \times 3 \times 1$, respectively. The convergence threshold was set as 10^{-4} eV for energy and 0.01 eV \AA^{-1} for force. To eliminate interactions between periodic structures, a vacuum of 20 Å was added. In this work, the typical (002) and (100) surfaces were selected for MoOS_x and CdS calculations, respectively. The Gibbs free energy of H atom adsorption (ΔG_{H^*}) was defined as following equation:

$$\Delta G_{\text{H}} = \Delta E_{\text{H}} + \Delta E_{\text{ZPE}} - T\Delta S_{\text{H}}$$

where ΔE_{H} , ΔE_{ZPE} , $T\Delta S_{\text{H}}$ are the differential hydrogen ΔE_{H} adsorption energy, the change in zero-point energy and entropy between the adsorbed hydrogen and molecular hydrogen in gas phase, respectively, and T is the temperature.

SI-4 The AQE calculation.

The apparent quantum efficiency (AQE) was evaluated according to the following equation:

$$\text{AQE [\%]} = \frac{\text{number of evolved H}_2 \text{ molecules} \times 2}{\text{number of incident photons}} \times 100\%$$

The average power of the light source (four 3-W 420±10 nm) was 27.3 mW/cm².

Thus, the AQE of the acquired few-layered MoOS_x/CdS(1 wt%) hollowsphere photocatalyst could be calculated to be 7.2 %.

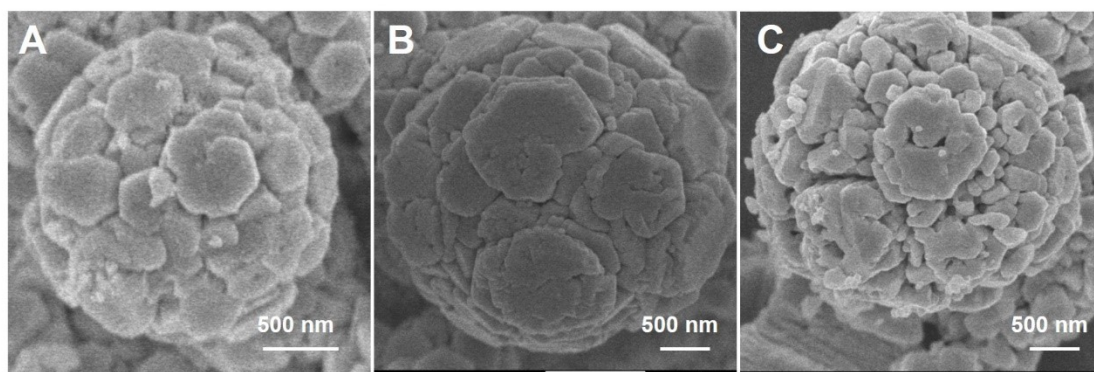


Fig. S1 FESEM images with different reaction time: (A) 1 h, (B) 8 h, and (C) 12 h.

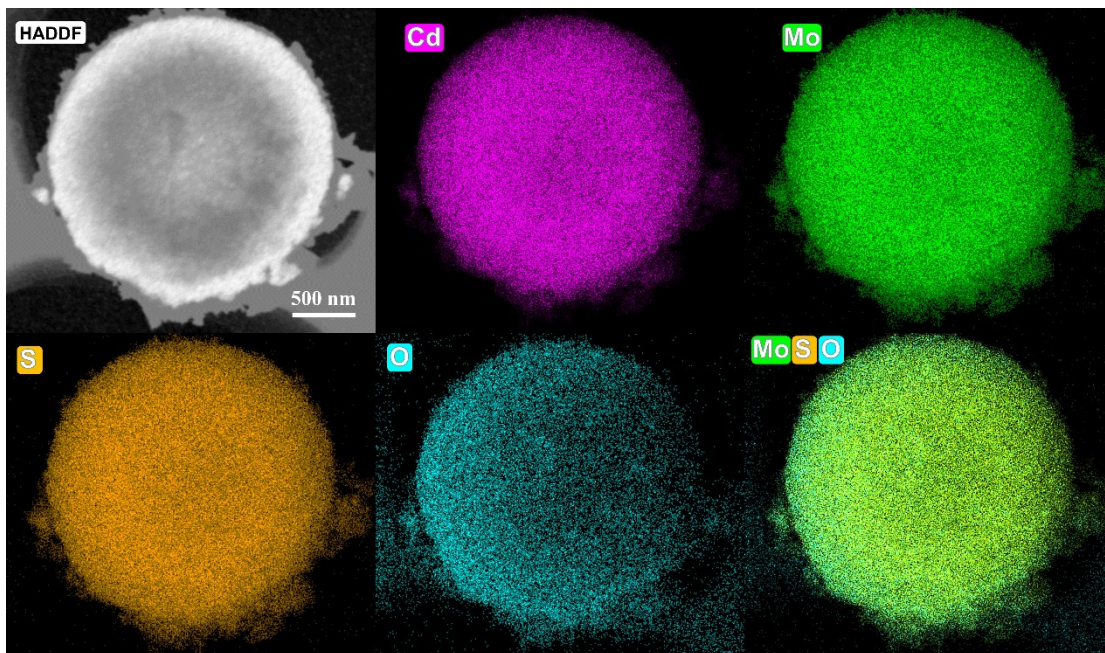


Fig. S2 HAADF-STEM and EDS images of few-layered MoOS_x/CdS hollowsphere photocatalyst.

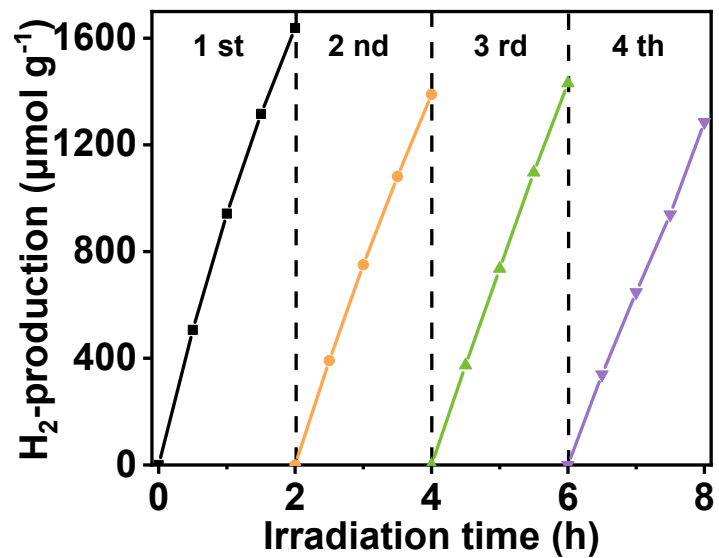


Fig. S3 Cycling photocatalytic H₂-evolution tests of the MoOS_x/CdS(1 wt%) photocatalyst.

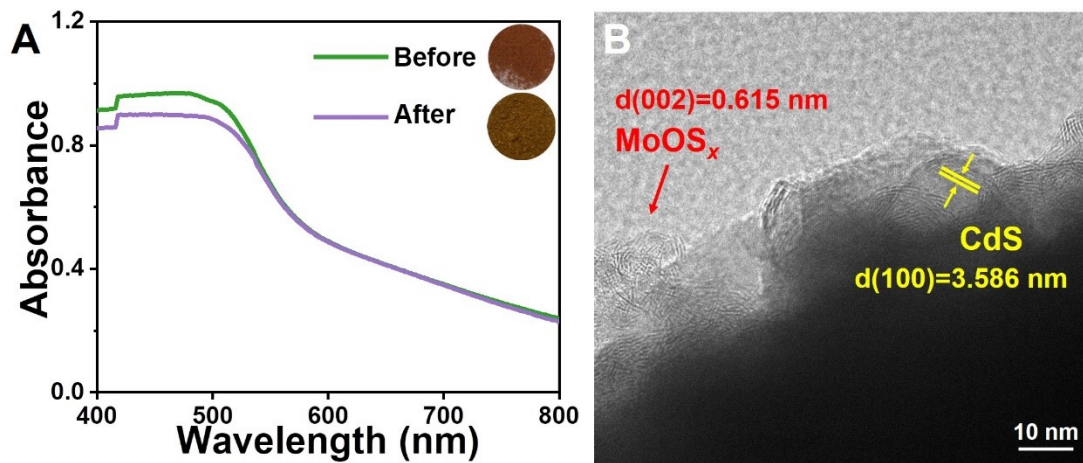


Fig. S4 (A) UV-vis absorption spectra of MoOS_x/CdS(1 wt%) photocatalyst before and after cycling experiments. (B) The corresponding TEM image of MoOS_x/CdS(1 wt%) photocatalyst after cycling experiments.

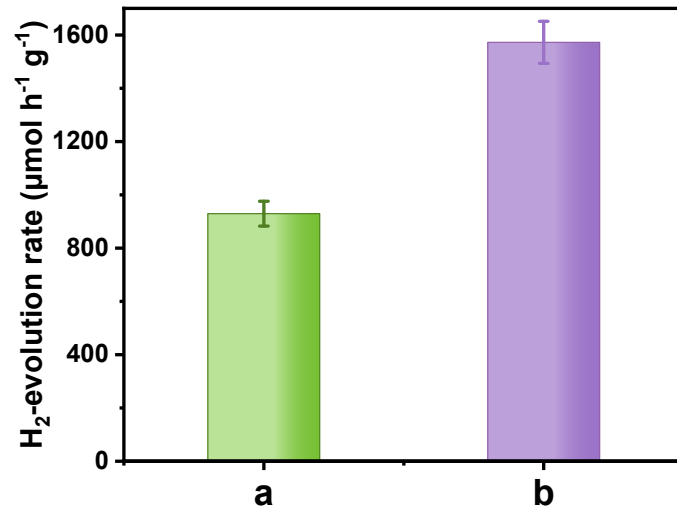


Fig. S5 The photocatalytic H₂-evolution rates of the (a) MoOS_x/CdS(1 wt%) and (b) Pt/CdS(1 wt%) photocatalysts.

Table S1. Comparison of the photocatalytic H₂-evolution rates for CdS based photocatalysts.

Photocatalysts	Light source	Sacrificial agent	Activity ($\mu\text{mol}\cdot\text{h}^{-1}\text{g}^{-1}$)	Ref.
MoOS _x /CdS	3-W 420 nm LED lamp	10 vol% lactic acid	929.4	This work
NiS/CdS	300 W Xe lamp	10 vol% lactic acid	542.0	[1]
CdS/g-C ₃ N ₄ /ZnFe ₂ O ₄	300 W Xe lamp	0.5 M Na ₂ SO ₃ -Na ₂ S	135.2	[2]
CdS@carbon dots	300 W Xe arc lamp	0.35 M Na ₂ SO ₃ -0.25 M Na ₂ S	344.0	[3]
CdS/VS ₂	300 W Xe lamp	0.25 M Na ₂ SO ₃ -0.35 M Na ₂ S	779.8	[4]
Ag ₂ S/CdS	300 W Xe lamp	2 vol% lactic acid	777.3	[5]
Ti ₃ C ₂ @CdS	300 W Xe lamp	20 vol% methanol	88.2	[6]
NaYF ₄ :Yb,Er/CdS	300 W Xe lamp	Na ₂ SO ₃ -Na ₂ S	2539	[7]
NiP _x /MoS ₂ /NiS/CdS	300 W Xe lamp	5 g/L glucose	297.0	[8]
CdS/NiO	300 W Xe lamp	0.25 M Na ₂ SO ₃ -0.35 M Na ₂ S	1770	[9]
CuO/CdS/CoWO ₄	300 W Xe lamp	0.5 M Na ₂ SO ₃ -Na ₂ S	457.9	[10]

References

- 1 Y. Yang, Q. Meng, X. Jiang, S. Meng, X. Zheng, S. Zhang, X. Fu and S. Chen, *ACS Appl. Energy Mater.*, 2020, **3**, 7736-7745.
- 2 R. Belakehal, K. Atacan, N. Güy, A. Megriche and M. Özacar, *Appl. Surf. Sci.*, 2022, **602**, 154315.
- 3 S. Qiu, Y. Shen, G. Wei, S. Yao, W. Xi, M. Shu, R. Si, M. Zhang, J. Zhu and C. An, *Appl. Catal. B Environ.*, 2019, **259**, 118036.
- 4 M. Niu, L. Cao, L. Feng, D. He, X. Li, Q. Chen, C. Fu and J. Huang,

- ChemNanoMat*, 2022, **8**, e202200163.
- 5 C. Lu, S. Du, Y. Zhao, Q. Wang, K. Ren, C. Li and W. Dou, *RSC Adv.*, 2021, **11**, 28211-28222.
 - 6 Y. Wang, X. Wang, Y. Ji, R. Bian, J. Li, X. Zhang, J. Tian, Q. Yang and F. Shi, *Int. J. Hydrogen Energy*, 2022, **47**, 22045-22053.
 - 7 H. Zhu, Y. Yang, Y. Kang, P. Niu, X. Kang, Z. Yang, H. Ye and G. Liu, *J. Mater. Sci. Technol.*, 2022, **102**, 1-7.
 - 8 X. Zheng, X. Wang, J. Liu, X. Fu, Y. Yang, H. Han, Y. Fan, S. Zhang, S. Meng and S. Chen, *J. Am. Ceram. Soc.*, 2021, **104**, 5307-5316.
 - 9 C. Deng, F. Ye, T. Wang, X. Ling, L. Peng, H. Yu, K. Ding, H. Hu, Q. Dong, H. Le and Y. Han, *Nano Res.*, 2021, **15**, 2003-2012.
 - 10 N. Güy, K. Atacan and M. Özacar, *Renewable Energy*, 2022, **195**, 107-120.